Original Article

Assessment of dynamic corneal nerve changes using static landmarks by *in vivo* large-area confocal microscopy—a longitudinal proof-of-concept study

Nadine Stache[1,2#], Katharina A. Sterenczak[1,2#], Karsten Sperlich[1,3], Carl F. Marfurt[4], Stephan Allgeier[5], Bernd Köhler[5], Ralf Mikut[5], Andreas Bartschat[5], Klaus-Martin Reichert[5], Rudolf F. Guthoff[1,3], Angrit Stachs[2], Oliver Stachs[1,3], Sebastian Bohn[1,3]

[1]Department of Ophthalmology, Rostock University Medical Center, Rostock, Germany; [2]Department of Obstetrics and Gynecology, University of Rostock, Rostock, Germany; [3]Department Life, Light & Matter, University of Rostock, Rostock, Germany; [4]Department of Anatomy Cell Biology & Physiology, Indiana University School of Medicine-Northwest, Gary, USA; [5]Institute for Automation and Applied Informatics, Karlsruhe Institute of Technology (KIT), Karlsruhe, Germany

Contributions: (I) Conception and design: A Stachs, O Stachs, S Bohn; (II) Administrative support: N Stache, KA Sterenczak, CF Marfurt, A Stachs, RF Guthoff; (III) Provision of study materials or patients: N Stache, KA Sterenczak, K Sperlich, A Stachs, O Stachs, S Bohn; (IV) Collection and assembly of data: N Stache, KA Sterenczak, K Sperlich, S Allgeier, B Köhler, R Mikut, A Bartschat, KM Reichert, S Bohn; (V) Data analysis and interpretation of data: N Stache, KA Sterenczak, CF Marfurt, O Stachs, S Bohn; (VI) Manuscript writing: All authors; (VII) Final approval of manuscript: All authors.

[#]These authors contributed equally to this work.

Correspondence to: Sebastian Bohn. Department of Ophthalmology, Rostock University Medical Center, Doberaner Straße 140, D-18057 Rostock, Germany. Email: sebastian.bohn@uni-rostock.de.

Background: The purpose of the present proof-of-concept study was to use large-area *in vivo* confocal laser scanning microscopy (CLSM) mosaics to determine the migration rates of nerve branching points in the human corneal subbasal nerve plexus (SNP).

Methods: Three healthy individuals were examined roughly weekly over a total period of six weeks by large-area *in vivo* confocal microscopy of the central cornea. An in-house developed prototype system for guided eye movement with an acquisition time of 40 s was used to image and generate large-area mosaics of the SNP. Kobayashi-structures and nerve entry points (EPs) were used as fixed structures to enable precise mosaic registration over time. The migration rate of 10 prominent nerve fiber branching points per participant was tracked and quantified over the longitudinal period.

Results: Total investigation times of 10 minutes maximum per participant were used to generate mosaic images with an average size of 3.61 mm^2 (range: 3.18–4.42 mm^2). Overall mean branching point migration rates of (46.4±14.3), (48.8±15.5), and (50.9±13.9) µm/week were found for the three participants with no statistically significant difference. Longitudinal analyses of nerve branching point migration over time revealed significant time-dependent changes in migration rate only in participant 3 between the last two measurements [(63.7±12.3) and (43.0±12.5) µm/week, $P<0.01$]. Considering individual branching point dynamics, significant differences in nerve migration rate from the mean were only found in a few exceptions.

Conclusions: The results of this proof-of-concept study have demonstrated the feasibility of using *in vivo* confocal microscopy to study the migration rates of corneal subbasal nerves within large areas of the central human cornea (>1 mm^2). The ability to monitor dynamic changes in the SNP opens a window to future studies of corneal nerve health and regenerative capacity in a number of systemic and ocular diseases. Since corneal nerves are considered part of the peripheral nervous system, this technique could also offer an objective diagnostic tool and biomarker for disease- or treatment-induced neuropathic changes.

Keywords: Large-area *in vivo* confocal laser scanning microscopy mosaics; corneal subbasal nerve plexus (SNP); migration rate of corneal subbasal nerves

Submitted Jan 07, 2022. Accepted for publication May 11, 2022.
doi: 10.21037/qims-22-15
View this article at: https://dx.doi.org/10.21037/qims-22-15

Introduction

The cornea is the most densely innervated tissue in the body (1). The cornea's transparency, accessible location on the anterior surface of the eye, and rich innervation make it an ideal candidate for imaging and monitoring health-related changes in the peripheral nervous system (2). In particular, the non-invasive *in vivo* visualization of the subbasal nerve plexus (SNP) is an important part of ophthalmological research (3) and has recently taken on expanded clinical significance. The most utilized non-invasive imaging method for *in vivo* visualization of structures of the human cornea is confocal laser scanning microscopy (CLSM) (4). CLSM is a relatively rapid, patient-friendly method of gaining high-resolution images of the corneal nerves and tracking their changes over time. CLSM has been used increasingly in recent years to quantify corneal nerve parameters such as density, tortuosity, and branching characteristics (4) in healthy eyes and in a large number of ophthalmological applications, including, dry eye treatment (5) and glaucoma therapy (6). Visualizing the SNP by CLSM has been used also as a diagnostic tool in various diseases affecting the nervous system, including, chronic migraine (7,8), trigeminal neuralgia (9), multiple sclerosis (10), familial amyloid neuropathy (11), Parkinson's disease (12), and polyneuropathy (13,14), especially diabetic polyneuropathy (15-17). Thereby, changes of the SNP could indicate changes of the nervous system itself, which could be monitored non-invasively over a long period by *in vivo* CLSM.

One important factor that has to be considered in any long-term investigation of corneal nerve anatomy is the dynamic nature of the SNP, resulting in structural changes. Auran *et al.* (18) were the first to report that the SNP was a dynamic structure and that individual subbasal nerves elongated, or migrated, continuously in the direction of the inferocentral whorl. Patel and McGhee (19) subsequently studied the centripetal migration of peripheral and central subbasal nerves over a 6-week period and observed that as the nerves approached the inferocentral whorl they rotated in a clockwise direction and their migration rate decreased. Within the whorl itself, the nerves degenerated and sloughed into the tear film (18). At the end of their six-week observation period, Patel and McGhee (19) noted that the overall pattern of the corneal SNP had changed noticeably. In a more recent study, Edwards *et al.* (20) also measured the migration rate of the corneal SNP with reference to the inferior whorl. They examined the corneas of two individuals with diabetes (one with and one without neuropathy) and of one healthy participant, at baseline and after 3 weeks. They concluded that diabetic neuropathy was associated with a reduced subbasal nerve migration rate (20). The aforementioned works all used the position of the inferocentral whorl and additional nerve landmarks located near the whorl as reference points for orientation (17,19,20). One potential limitation of this method is the manual and inaccurate selection of landmarks (21), especially in non-whorl regions of the peripheral cornea where stable landmarks are harder to define (19).

The goal of the present proof-of-concept study was to assess the feasibility of using large area SNP mosaics (22,23) to study SNP migration in central corneal areas outside of the inferocentral whorl. As landmarks, Kobayashi-structures (K-structures) (24,25), which occur after pressure on the ocular surface at the level of the SNP and entry points (EPs) of nerves emerging from Bowman's layer into the epithelium (18), were utilized. K-structures which represent polymorphic ridge-like structures composed of fibrillary materials were reported to strongly align with the anterior corneal mosaic (ACM) (26) and the authors hypothesized that K-structures represent the structural basis for ACM formation (25). Auran *et al.* (18) have shown previously that landmarks such as the ACM and EPs remain fixed in position over time and consequently could be used as reliable orientation structures for the assignment of identical areas in the mosaic images taken at different sessions during the present proof-of-concept study in order to study the dynamics of SNP migration. We present the following article in accordance with the MDAR checklist (available at https://qims.amegroups.com/article/view/10.21037/qims-22-15/rc).

Methods

Participants

Images used in this analysis were obtained from the central corneal zones of three healthy participants. The details about sex and age are as follows: participant 1 – male, 55 y.o.; participant 2 – female, 42 y.o.; participant 3 – male, 28 y.o. Participants had no history of eye disease or systemic disease that may have affected the cornea and no known history of contact lens wear. The study was conducted in accordance with the Declaration of Helsinki (as revised in 2013). The study was approved by the Institutional Review Board of Rostock University Medical Center [No. A 2018-0162 (dated 23 August 2018)]. All participants consented to large-area imaging of their corneas by *in vivo* CLSM in six separate sessions performed at roughly weekly intervals. The exact time between the investigations ranged from 6 to 10 days, as is clearly specified in the Results section. Except for two investigations of participant 2, all investigations were performed by the same examiner.

Image acquisition

CLSM images were recorded from the human corneal SNP using a Heidelberg Retina Tomograph 3 (HRT3, Heidelberg Engineering GmbH, Heidelberg, Germany) in conjunction with a modified Rostock Cornea Module, called Rostock Cornea Module 2.0 (RCM 2.0) (27,28), and the EyeGuidance system (22,23). CLSM was performed on the left eyes of all participants over a total period of six weeks.

Using the RCM 2.0, the internal objective lens can be moved by the additionally equipped piezo actuator (MIPOS 600 SG DIG, Piezosystem Jena GmbH, Jena, Germany). The EyeGuidance System uses a smartphone (Motorola Moto G, Motorola Mobility Germany GmbH, Idstein, Germany) with an Android operating system and presents a computer-controlled fixation target to the contralateral eye (29,30). Since both eyes move in unison, the EyeGuidance system enables controlled movement of the examined eye during CLSM imaging (29,30). A customized HRT software was used providing the possibility to record an unlimited image stream at 30 frames per second and a network-based communication interface.

For preparation, the cornea of each participant was anesthetized with Proparakain-POS® 0.5% eye drops (Ursapharm, Saarbrücken, Germany), and Vidisic Gel (Bausch & Lomb/Dr. Mann Pharma, Berlin, Germany) was applied as a coupling medium between the objective lens and contact cap (TomoCap, Heidelberg Engineering, Heidelberg, Germany) as well as between TomoCap and the participant's cornea. To start the investigation, it was essential to position the participant with the head in the forehead support and the chin on the chin support in a secure manner that prohibits the head from moving while processing images. After positioning, the operator places the EyeGuidance system in front of the non-examined eye and conventionally adjusts the HRT. After locating the central cornea, the custom image acquisition mode "Streaming Mode" can be started automatically with the start button. The examined eye moves along a spiraling pattern visualized in the contralateral eye by the EyeGuidance system at a defined speed while the piezo drive of the RCM 2.0 oscillates the focal plane with a constant speed of 120 µm/s and amplitude of ±20 µm centered on the SNP. This focal plane oscillation is used to acquire a volumetric dataset that is guaranteed to contain sufficient SNP images for mosaicking. The subsequent automatic process for generating large-area SNP mosaic images with the RCM 2.0 and the EyeGuidance system was described in detail previously (23,29,30).

The amount of pressure was adjusted in such a way that K-structures are clearly visible in the CLSM images. Here, it is not important to obtain the same K-structures. Only some degree of formation of tissue fold is needed in order to recognize the same K-structures features. If parts of the epithelium or stroma can be seen in the SNP due to the induced tissue folds, the pressure is already considerably higher than necessary.

Specification of reference points

By referencing K-structures and EPs, it was possible to identify the same regions in the SNP mosaics week after week. K-structures, first described by Kobayashi *et al.* (24,25), are anterior collagen fiber bundles located just beneath Bowman's membrane that appear as ridges and striae after the application of pressure by a TomoCap. The K-structure network matches the pattern of the ACM formation (24,26), and we hypothesize that these structures might represent an individual corneal "fingerprint" that persists over time.

To confirm that K-structures and EPs do not change their location over time, two separate SNP mosaics of one of the participants in this study were acquired at the inferocentral whorl region 253 days apart. In these images,

prominent locations of K-structures and EPs present in both mosaics were searched for, and their distance to each other and to the center of the whorl was measured. Based on these K-structures and EPs, reference points were marked within the SNP enabling the registration of both SNP mosaics using the control point registration (CPR) procedure provided by MATLAB's Image Processing Toolbox (MATLAB, MathWorks Inc., USA). With CPR, a set of multiple matching control point pairs are selected in two mosaics. Then, a transformation matrix combining translation, rotation, and scaling is estimated to register these mosaics.

Measurement of nerve migration

Since nerve migration rates have been reported to be different in the central and peripheral cornea (20), it is important to draw a comparison to previous work. Therefore, the distance from the center of the inferocentral whorl to our region of interest, which was the central region of the cornea, was determined for one participant. For this purpose, a mosaic around the whorl was registered to a mosaic in the center using CPR.

One of the 6 weekly mosaics from each participant was chosen as the fixed image and the remaining 5 were registered to it by CPR. By visual inspection, this reference image was selected based on various, but not strict, criteria: a large area, a sufficient number of landmarks that are also found in the other images, and a central location relative to the other images. Over the six weeks, 10 SNP branching points (BPs) were selected. To derive an individual migration rate of the SNP, the mean and standard deviation (SD) of BP movement per week for all 10 BPs on every date of the six weeks was calculated. For further analysis, the mean values and SDs of BP movement per week over all measured BPs at each individual date and at each individual BP over all dates were calculated.

Statistical analysis

For statistical analysis, migration rates were tested for significant differences. First, each participant was considered as one group and tested whether there were significant differences between their migration rates. Then, per participant, it was tested whether there were significant differences with respect to the measurement dates or the individual BPs.

At first, the data sets were tested for normal distribution using the Anderson-Darling test. Depending on the results, a one-way analysis of variance (ANOVA) was then performed as a parametric test or the Kruskal-Wallis test as a nonparametric test. If this revealed significant differences, pairwise comparisons via the Bonferroni method were conducted to test which groups had significant differences.

Results

Approach for large-area CLSM

Using this technique, mosaic images with an average size of 3.61 mm^2 were obtained. The smallest and largest images were 3.37 and 3.74 mm^2 respectively, for participant 1, 2.96 and 3.99 mm^2 for participant 2, and 3.18 and 4.42 mm^2 for participant 3.

Landmarks and localization

Figure 1 shows an example of the analysis made using CPR. Two mosaics of one participant from the 7^{th} and 36^{th} day of the measurement campaign are shown in *Figure 1A*,*1B*, respectively. In order to find the same region, K-structures and EPs found in both mosaics were used as a reference. Six matching control point pairs were selected in this case. *Figure 1C* shows magnified images of the same area in the two mosaics in which the same "K-structure" can be seen; single EPs were chosen as control point pairs. Finally, *Figure 1D* shows a composite false-color image of both mosaics from *Figure 1A*,*1B* after image registration using CPR. In the false-color representation, structures that are in the same position in both images are displayed in shades of gray. Thus, matching K-structures and EPs, as well as the movement of the SNP nerve fibers, are clearly discernible.

Evidence that the K-structures and EPs do not change their locations within the cornea over time is illustrated in *Figure 2*. In the mosaics shown in *Figure 2A*,*2B*, the locations of two prominent K-structures and EPs are marked. The distances between these landmark structures and to the whorl did not change with time (t=253 days).

Figure 2C shows a false-color composite consisting of the mosaic from *Figure 2B* and a central corneal mosaic acquired at an earlier session during the presented study. The central corneal mosaic was recorded 128 days after the mosaic shown in *Figure 2A* and 125 days before the mosaic shown in *Figure 2B*. Here it becomes even more apparent that the ACM does not change its pattern over time. The spatial distance between the inferocentral whorl and the center

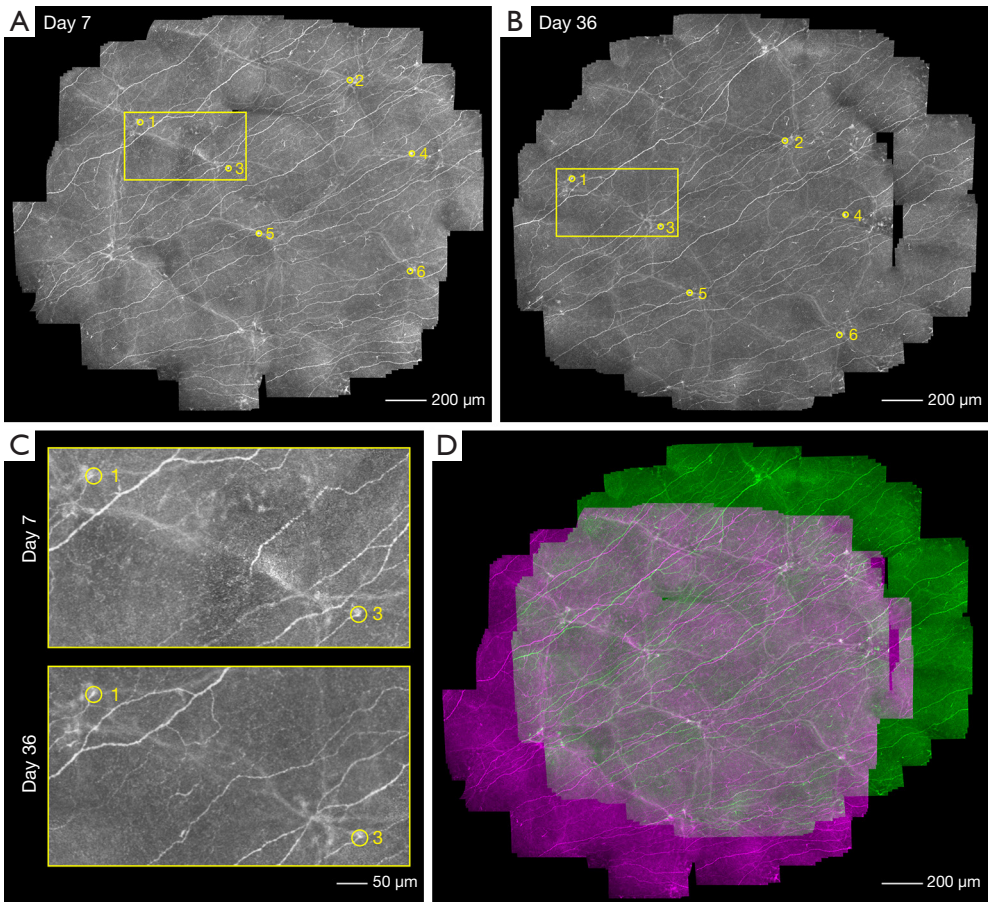

Figure 1 Example of control point registration. (A,B) Two mosaics of the central cornea in the same participant but at different acquisition times (29 days apart). Yellow circles mark the same structures as control points that do not change their relative position to the K-structures and entry points. (C) Magnified section showing entry points as control points. (D) Composite false-color image of the mosaic images registered by CPR. K-structures, Kobayashi-structures; CPR, control point registration.

of the cornea as the region of interest is about 1.8 mm, which is consistent with the observation that the whorl is located 1–2 mm inferior and nasal to the corneal apex.

Residual image size after registration and longitudinal fusion

The residual image size is the overlapping area of the six weekly mosaics after registration. For participants 1, 2, and 3, the residual image size was 1.85, 1.86, and 1.14 mm^2, respectively. All of the tracked BPs were located within the residual area for all participants.

Overall branching point dynamics

The analyses of branching point dynamics are depicted in *Figure 3*, *Figure 4*, and *Figure 5* for participants 1, 2, and 3, respectively. *Figure 3A*, *Figure 4A*, and *Figure 5A* illustrate the movements of 10 BPs over six weeks from participants 1, 2, and 3, respectively. The mean rate of BP movement in the three corneas was (46.4±14.3), (48.8±15.5), and (50.9±13.9) µm/week, respectively. One-way ANOVA revealed that the difference in mean migration rates for all BPs at each time point in all three corneas showed no statistical significance to each.

Longitudinal changes in branching point dynamics

When comparing the rates of BP movement at each individual measurement date, no significant differences were observed for participants 1 and 2 (*Figure 3B* and *Figure 4B*). In contrast, in participant 3, a significant difference ($P<0.01$) between

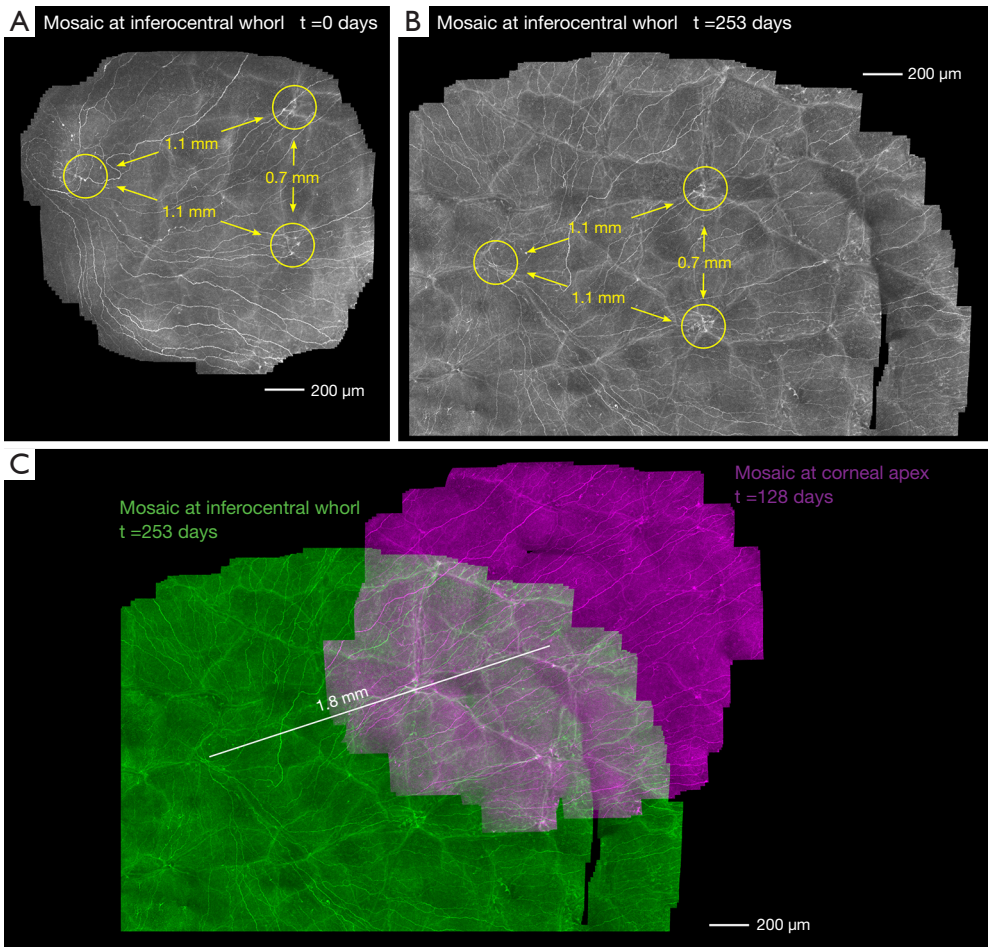

Figure 2 Location of K-structures and subbasal nerve entry points in relation to the inferocentral whorl. (A,B) Two mosaics of the inferocentral whorl in the same eye but at different acquisition times (253 days apart). Yellow circles mark the whorl and same distinct locations of K-structures and entry points in both mosaics. The distance between each marked area and the others does not change over time. (C) Composite false-color image registered by CPR consisting of the mosaic from B (green) and a central corneal mosaic acquired 128 days after A and 125 days before B (purple). The distance of 1.8 mm is measured from the inferocentral whorl to the region of interest. K-structures, Kobayashi-structures; CPR, control point registration.

the movement from day 21 to 29 at (63.7±12.3) µm/week and from day 29 to 36 at (43.0±12.5) µm/day was observed (*Figure 5B*).

Individual branching point dynamic

Analyses of the migration rates of individual BPs revealed for participant 1 significant differences between BP 2 and BP 3 ($P<0.05$), between BP 3 and BP 7 ($P<0.01$), and between BP 7 and BP 8 ($P<0.05$), see *Figure 3C*. BPs 2 and 7 showed faster movement at (59.8±11.6) and (65.9±13.3) µm/week, respectively, whereas BPs 3 and 8 showed slower movements at (33.3±6.1) and (33.4±11.1) µm/week, respectively. For participant 2, statistical analysis revealed significant differences in the movement of individual BPs between BP 5 and BP 7 ($P<0.05$) and between BP 5 and BP 10 ($P<0.05$), see *Figure 4C*. While BP 7 and 10 in participant 2 moved at slower rates of respectively (33.9±13.7) and (35.5±14.2) µm/week, BP 5 exhibited the fastest rate of movement seen in this study at (68.2±5.8) µm/week. In participant 3, no significant differences occurred in the movement of single BPs (*Figure 5C*).

Figure 6 depicts in participant 2 a set of EPs and the movement of BPs 2, 5, and 9 in an area of the SNP mosaic

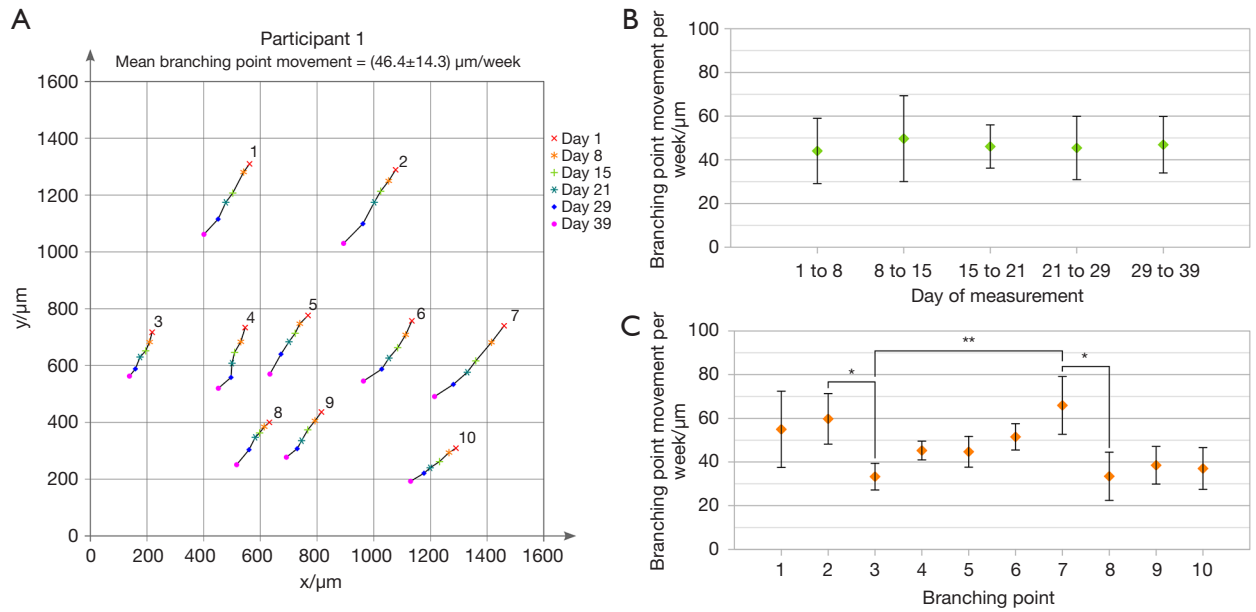

Figure 3 Analysis of branching point dynamics for participant 1. (A) Ten tracked SNP branching points of participant 1 after registration of SNP mosaics acquired over six weeks. The mean and SD of branching point movement per week were calculated for all branching points on every date. (B) Mean values and SDs of branching point movement per week at each individual date for all branching points. (C) Mean values and SDs of branching point movement per week for each individual branching point over all dates. Statistical significance: P<0.05 (*) and P<0.01 (**). SNP, subbasal nerve plexus; SD, standard deviation.

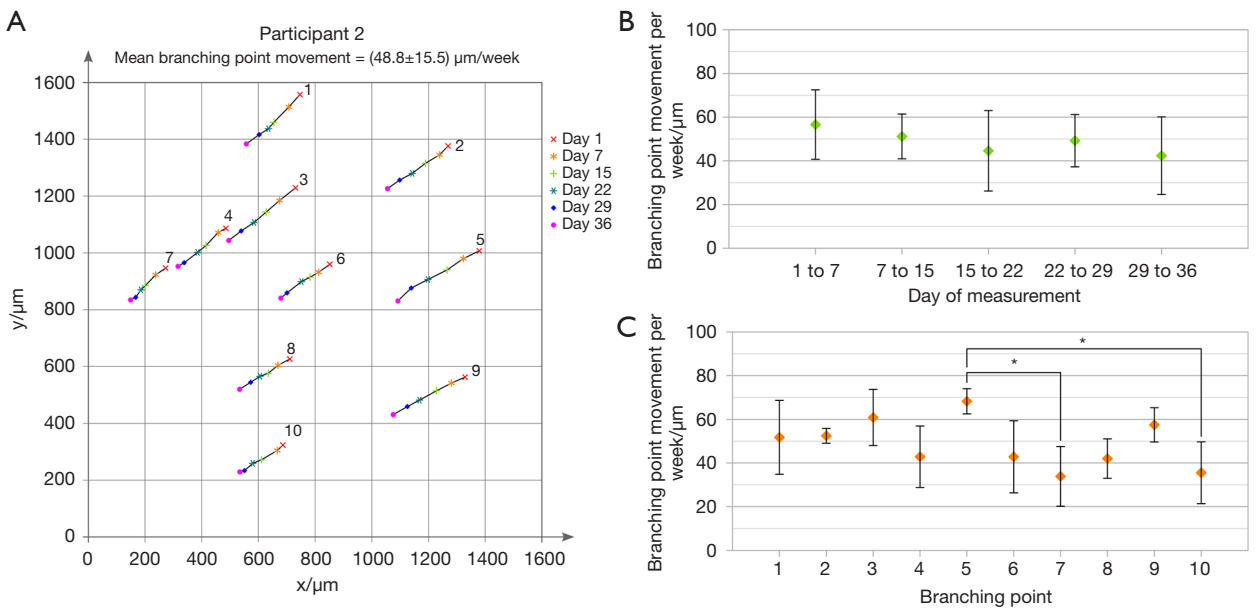

Figure 4 Analysis of branching point dynamics for participant 2. (A) Ten tracked SNP branching points of participant 2 after registration of SNP mosaics acquired over six weeks. The mean and SD of branching point movement per week were calculated for all branching points on every date. (B) Mean values and SDs of branching point movement per week at each individual date for all branching points. (C) Mean values and SDs of branching point movement per week at each individual branching point over all dates. Statistical significance: P<0.05 (*). SNP, subbasal nerve plexus; SD, standard deviation.

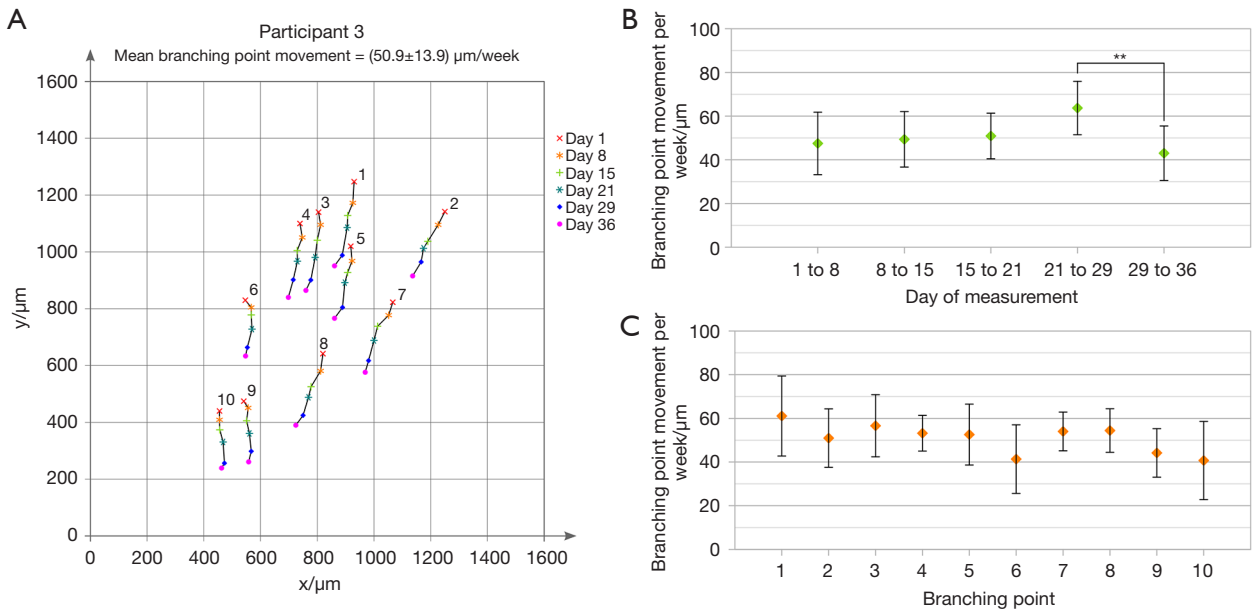

Figure 5 Analysis of branching point dynamics for participant 3. (A) Ten tracked SNP branching points of participant 3 after registration of SNP mosaics acquired over six weeks. The mean and SD of branching point movement per week were calculated for all branching points on every date. (B) Mean values and SDs of branching point movement per week at each individual date for all branching points. (C) Mean values and SDs of branching point movement per week at each individual branching point over all dates. Statistical significance: P<0.01 (**). SNP, subbasal nerve plexus; SD, standard deviation.

at different examination dates. While the EPs remain fixed in place, the BPs move in the direction of the nerve fiber progression towards the inferocentral whorl.

Discussion

The technique described in this article offers an efficient method to image the SNP and measure corneal subbasal nerve migration rates in whole corneas. Due to high-resolution images, the same structures were easy to reidentify between various times and could be compared with each other. In the past, this tool was already used for longitudinal research on a breast cancer patient during Trastuzumab and Paclitaxel treatment (31). In previous CLSM studies of SNP migration, the inferocentral whorl was used as a landmark (18-20). Patel and McGhee (19) obtained results up to 698 µm from the whorl, while Edwards *et al.* (20) were able to measure migration rates at distances up to about 3.7 mm from the whorl. In contrast, by using K-structures as landmarks in the current investigation, it is theoretically possible to explore the whole cornea and obtain results even in peripheral and perilimbal zones. The exploration of the corneal SNP is not confined to the region of the whorl because K-structures can be induced everywhere on the cornea by pressure and are easy to re-identify. Furthermore, since the inferocentral whorl is a rather diffuse region that no specific singular point can be assigned to, using multiple landmarks such as K-structures and EPs, the detection of nerve changes and their migration speed is more precise and can be observed over long periods.

Utilizing K-structures and EPs to select reference points for CPR enables reliable registration results. Theoretically, there should be no scaling needed between two mosaics; however, this assumes that the control point pairs are chosen perfectly and the SNP mosaics are generated completely without distortions. In the edge region of the SNP mosaics, this is not always guaranteed, since information for the registration of surrounding images may be missing. If control points are located in these edge regions, deviations can occur. Nevertheless, in this study, the largest changes in scale were smaller than 3% and mostly smaller than 1%. In comparison to the average mosaic image size, the residual image size after registration and longitudinal fusion of six weekly mosaics resulted in an overlapping area of 50% for participants 1 and 2, while

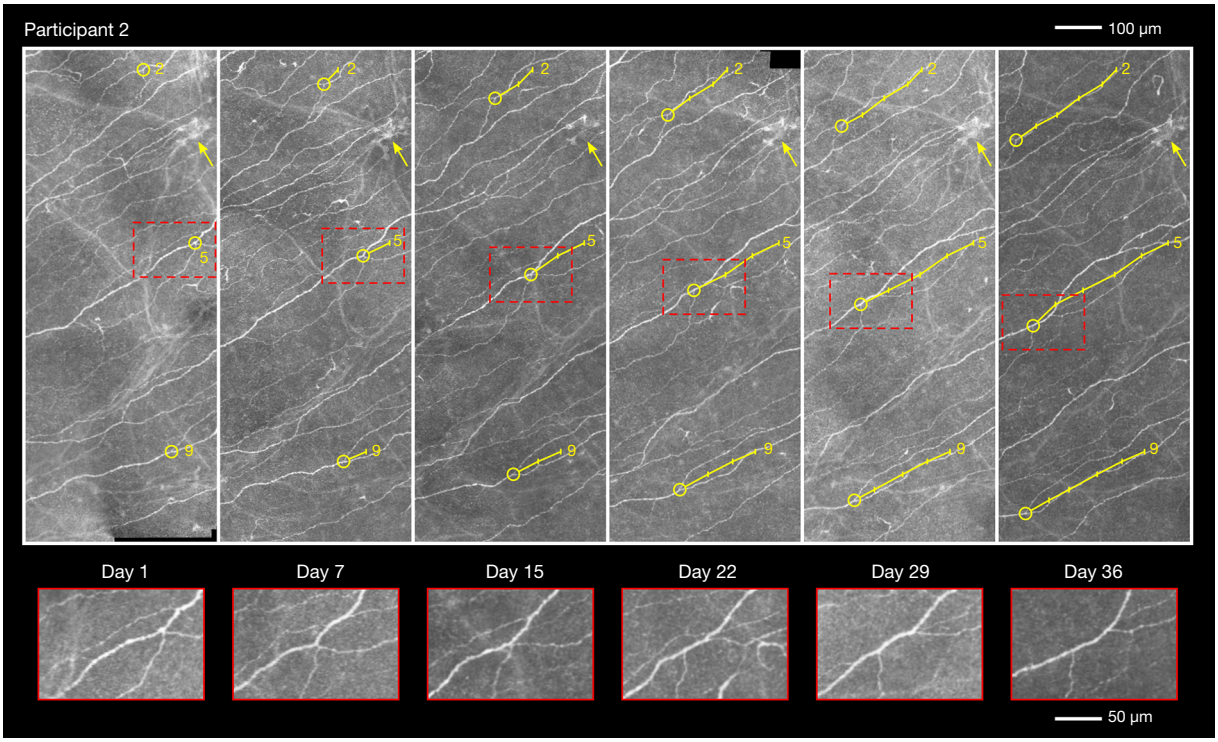

Figure 6 Selected branching point movements in participant 2 at roughly weekly intervals, as seen in high-magnification images of the respective mosaics. The numbering of branching points corresponds to that in Figure 4. Arrows show a set of entry points that do not change in position. The movement of branching point 5 (red rectangle in top images) is shown at higher magnification in the insets at the bottom.

for participant 3 it was reduced to around 30%. The latter was due to non-optimal relocalization of the same location within the cornea. However, this was still sufficient to track ten BP over six weeks. With the help of K-structures and EPs, subbasal nerve fibers are precisely recognized and even the influence of rotation of SNP mosaics (e.g., as might be caused by different seating positions of the participants) is considered. Consequently, minor differences in starting conditions of measurement in the regions of concern do not influence the results. Even after intervals of greater than one year between investigations (not shown here), it is possible to recognize the same nerve fibers. Furthermore, due to the exceptional repeatability of the method, the use of different investigators does not affect the results, a conclusion also derived previously by Al Rashah *et al.* (32).

Some other studies exist that used large-scale CLSM images of the SNP to compare healthy and treatment groups and examine differences over time. For example, Chao *et al.* (33,34) examined differences in the SNP before and after laser-assisted *in situ* keratomileusis, and Lum *et al.* (35,36) investigated changes in the SNP morphology during orthokeratology. All these mentioned studies used 1 mm^2 CLSM images of the central and peripheral cornea. Examinations such as those of Chao *et al.* and Lum *et al.* always bear the risk that the precise location of the analyzed area varies between longitudinally repeated examinations. By eliminating this potential source of bias, similar studies could benefit from using K-structures and EPs as absolute positional landmarks in terms of increased accuracy.

Previous studies have shown that the SNP migration rate is dependent on distance from the inferocentral whorl (18-20). Edwards *et al.* (20) used linear equations to estimate nerve migration rates in the central cornea of 46.7, 46.1, and 22.2 µm/week in a healthy control participant, a Type 1 Diabetes patient without neuropathy, and a Type 1 Diabetes patient with neuropathy, respectively. Our results of 46.4, 48.8, and 50.9 µm/week in three healthy volunteers, at a distance of approximately 1,800 µm from the center of the whorl, agree well with the migration rates of the control participant and the Type

1 Diabetes patient without neuropathy in the study by Edwards and coworkers (20). Al Rashah *et al.* (37) also measured SNP migration rates at an average distance of 1,200±50 µm from the inferocentral whorl region in volunteers from three different age groups, and reported rates of 42.0±14.0, 42.3±15.5, and 42.0±10.8 µm/week, respectively. The nerve migration rates reported in the current investigation, assessed at a distance of approximately 1.8 mm from the inferocentral whorl (see *Figure 2C*), are comparable to those detected by Al Rashah and coworkers as well.

In participant 2 of the present study, BP 5 was observed to move the fastest compared to the others. From day 22 onwards, this fast-moving BP underwent an additional, secondary branching event during the course of the investigation and split into two BPs (see *Figure 6*), which could be the reason for its putative faster movement. This reinforces the notion that BPs are as dynamic as the nerve fibers themselves. It is tempting to speculate that splitting (divergence) or fusion (convergence) of subbasal nerve fibers at branch points may exert temporal influences on nerve migration rate and that these types of morphological changes should be considered when selecting nerve fibers for analysis in CLSM investigations of this type.

The average nerve migration rates observed in the three participants of our investigation were remarkably similar and there were no significant differences. Al Rashah *et al.* (37) similarly reported that nerve migration rate seems not to be affected by age, sex, BMI, nicotine, or alcohol abuse, although they did find a positive correlation between nerve migration rate and physical activity. Interestingly, in participant 3 in the present study, nerve migration speed accelerated appreciably during one of the examination intervals (day 21 to 29). At the present time, the underlying effects are completely unknown and consequently, in the future additional investigations analyzing the influence of various criteria like illness, psychological and physiological stressors, general and current physical activities, or genetic factors should be implemented.

In summary, there seems to be good accordance between the measured migration rates of this study and the values of independent groups (19,20,37), which supports the notion of a meaningful reference value for the migration rate. Since this parameter can be influenced by certain circumstances, it can be hypothesized that the migration rate could act as a biomarker for different types of conditions (19).

The presented method opens a window for future *in vivo* investigations of corneal nerves allowing accurate corneal global mapping in order to study nerve migration. This powerful tool enables a "survey" view of the overall corneal nerve pattern, and by referencing K-structures and EPs, BPs can be identified aiding in the accurate detection of changes over time. While Patel and McGhee acquired at least 800 images per session in a duration of about 50 min (19) and Edwards *et al.* required 15–20 min per examination (17), it takes only 40 s with the EyeGuidance system used here to capture images that result in mosaics with an average size of 3.6 mm^2. Altogether up to 5 to 10 min per participant were needed for preparation, depending on the experience of the examiner and the participant's convenience and compliance. Furthermore, EyeGuidance offers a live preview of the resulting mosaic and allows for simultaneous evaluation during scanning of the quality, size, and location of the mosaic (30). This is a breakthrough improvement making clinical studies actionable and reasonable even for investigations of patients with compromised health status. Accordingly, patients' compliance is increased and potential limitations like dry eye and blurred vision due to long examination duration (19) can be avoided, which is especially important for patients with ocular surface diseases.

In comparison to standard morphological SNP parameters, e.g., corneal nerve fiber density, corneal nerve branch density, or corneal nerve fiber length, the migration rate represents a dynamic parameter and its determination is not as prone to error, as it does not depend on the imaging quality of whole nerves without distortions and interruptions. Nonetheless, a limiting factor is that recordings on at least two different days with sufficient distance are necessary. Moreover, it must be considered that morphology and dynamics represent different quantities and the detection of identical areas is ambitious and needs effort in technology and experience. In the future, studies will be needed to validate the significance of dynamic parameters such as migration speed. Furthermore, it will be necessary to investigate the correlation between static and dynamic properties.

In conclusion, detecting the migration rate of corneal subbasal nerves by large-area confocal microscopy and the use of static landmarks such as K-structures and EPs offers a novel and unique opportunity to obtain more information about corneal nerve changes and potential nerve regeneration in, e.g., patients with diabetic neuropathy (37), cytostatic induced neuropathy, keratoconus (19), and many other ophthalmologic and systemic conditions. More broadly, observing the dynamic SNP by CLSM might be a

helpful diagnostic tool and a potential objective biomarker for clinical investigations of changes in the peripheral nervous system as a whole, such as in small fiber neuropathy due to, for example, diabetes (20) or chemotherapy-induced peripheral neuropathy in patients suffering from cancer. Therefore, basic information about the longitudinal behavior of corneal nerves in healthy individuals such as presented here could have great clinical significance for future studies. SNP migration rate could provide a novel diagnostic criterion leading to early therapy adjustment by tracking disease progression or treatment-related changes, and ultimately, leading to a possible improvement of the outcome and quality of life. Although only three subjects were examined in this proof-of-concept study, the authors are confident that the generalizability of the novel method presented can be confirmed in a larger cohort. A study with a larger sample size in which, among other things, the migration rate will be measured is the subject of future research.

Acknowledgments

The authors would like to thank the whole team of the Department of Ophthalmology and Department Life, Light & Matter at the University Rostock (Rostock, Germany) for support and numerous fruitful discussions. The authors also acknowledge financial support by Deutsche Forschungsgemeinschaft and Universität Rostock/Universitätsmedizin Rostock within the funding program Open Access Publishing.

Funding: This work was funded by the Deutsche Forschungsgemeinschaft (DFG, German Research Foundation) (grant numbers: STA 543/6-2, STA 543/9-1, MI 1315/5-2, KO 5003/1-2, and INST 264/190-1 FUGG) and the German Federal Ministry of Education and Research (Antifibrotix, 03VP06230; RESPONSE "Partnership for Innovation in Implant Technology").

Footnote

Reporting Checklist: The authors have completed the MDAR checklist. Available at https://qims.amegroups.com/article/view/10.21037/qims-22-15/rc

Conflicts of Interest: All authors have completed the ICMJE uniform disclosure form (available at https://qims.amegroups.com/article/view/10.21037/qims-22-15/coif). KAS, RFG, and OS report grants from the German Federal Ministry of Education and Research outside the submitted work. KS, SA, BK, RM, AB, OS and SB report grants from Deutsche Forschungsgemeinschaft (DFG, German Research Foundation) during the conduct of the study. The other authors have no conflicts of interest to declare.

Ethical Statement: The authors are accountable for all aspects of the work in ensuring that questions related to the accuracy or integrity of any part of the work are appropriately investigated and resolved. The study was conducted in accordance with the Declaration of Helsinki (as revised in 2013). The study was approved by the Institutional Review Board of Rostock University Medical Center [No. A 2018-0162 (dated 23 August 2018)], and informed consent was obtained from all subjects before enrollment.

References

1. Nguyen KH, Patel BC, Tadi P. Anatomy, Head and Neck, Eye Retina 2022. Treasure Island (FL): StatPearls Publishing, 2022.
2. Argyriou AA, Park SB, Islam B, Tamburin S, Velasco R, Alberti P, Bruna J, Psimaras D, Cavaletti G, Cornblath DR; Toxic Neuropathy Consortium (TNC). Neurophysiological, nerve imaging and other techniques to assess chemotherapy-induced peripheral neurotoxicity in the clinical and research settings. J Neurol Neurosurg Psychiatry 2019;90:1361-9.
3. Winter K, Scheibe P, Guthoff RF, Allgeier S, Stachs O. Morphometric characterization of the subbasal nerve plexus : Detection and analysis of networks of nerve fibers. Ophthalmologe 2017;114:608-16.
4. De Silva MEH, Zhang AC, Karahalios A, Chinnery HR, Downie LE. Laser scanning in vivo confocal microscopy (IVCM) for evaluating human corneal sub-basal nerve plexus parameters: protocol for a systematic review. BMJ Open 2017;7:e018646.

5. Iaccheri B, Torroni G, Cagini C, Fiore T, Cerquaglia A, Lupidi M, Cillino S, Dua HS. Corneal confocal scanning laser microscopy in patients with dry eye disease treated with topical cyclosporine. Eye (Lond) 2017;31:788-94.
6. Mastropasqua L, Agnifili L, Fasanella V, Curcio C, Ciabattoni C, Mastropasqua R, Toto L, Ciancaglini M. Conjunctival goblet cells density and preservative-free tafluprost therapy for glaucoma: an in vivo confocal microscopy and impression cytology study. Acta Ophthalmol 2013;91:e397-405.
7. Shetty R, Deshmukh R, Shroff R, Dedhiya C, Jayadev C. Subbasal Nerve Plexus Changes in Chronic Migraine. Cornea 2018;37:72-5.
8. Shen F, Dong X, Zhou X, Yan L, Wan Q. Corneal subbasal nerve plexus changes in patients with episodic migraine: an in vivo confocal microscopy study. J Pain Res 2019;12:1489-95.
9. Lee JI, Böcking T, Holle-Lee D, Malik RA, Kieseier BC, Hartung HP, Guthoff R, Kleinschnitz C, Stettner M. Corneal Confocal Microscopy Demonstrates Corneal Nerve Loss in Patients With Trigeminal Neuralgia. Front Neurol 2020;11:661.
10. Bitirgen G, Akpinar Z, Malik RA, Ozkagnici A. Use of Corneal Confocal Microscopy to Detect Corneal Nerve Loss and Increased Dendritic Cells in Patients With Multiple Sclerosis. JAMA Ophthalmol 2017;135:777-82.
11. Zhang Y, Liu Z, Zhang Y, Wang H, Liu X, Zhang S, Liu X, Fan D. Corneal sub-basal whorl-like nerve plexus: a landmark for early and follow-up evaluation in transthyretin familial amyloid polyneuropathy. Eur J Neurol 2021;28:630-8.
12. Che NN, Yang HQ. Potential use of corneal confocal microscopy in the diagnosis of Parkinson's disease associated neuropathy. Transl Neurodegener 2020;9:28.
13. Koschmieder A, Stachs O, Kragl B, Stahnke T, Sterenczak KA, Henze L, Jünemann AG, Junghanss C, Guthoff RF, Murua Escobar H. Non-invasive detection of corneal sub-basal nerve plexus changes in multiple myeloma patients by confocal laser scanning microscopy. Biosci Rep 2020;40:BSR20193563.
14. Ferdousi M, Azmi S, Petropoulos IN, Fadavi H, Ponirakis G, Marshall A, Tavakoli M, Malik I, Mansoor W, Malik RA. Corneal Confocal Microscopy Detects Small Fibre Neuropathy in Patients with Upper Gastrointestinal Cancer and Nerve Regeneration in Chemotherapy Induced Peripheral Neuropathy. PLoS One 2015;10:e0139394.
15. Roszkowska AM, Licitra C, Tumminello G, Postorino EI, Colonna MR, Aragona P. Corneal nerves in diabetes-The role of the in vivo corneal confocal microscopy of the subbasal nerve plexus in the assessment of peripheral small fiber neuropathy. Surv Ophthalmol 2021;66:493-513.
16. Badian RA, Utheim TP, Lagali N. Region of interest and directional analysis of subbasal nerves in wide-area corneal nerve plexus mosaics in type 2 diabetes mellitus. Sci Rep 2020;10:10802.
17. Edwards K, Pritchard N, Gosschalk K, Sampson GP, Russell A, Malik RA, Efron N. Wide-field assessment of the human corneal subbasal nerve plexus in diabetic neuropathy using a novel mapping technique. Cornea 2012;31:1078-82.
18. Auran JD, Koester CJ, Kleiman NJ, Rapaport R, Bomann JS, Wirotsko BM, Florakis GJ, Koniarek JP. Scanning slit confocal microscopic observation of cell morphology and movement within the normal human anterior cornea. Ophthalmology 1995;102:33-41.
19. Patel DV, McGhee CN. In vivo laser scanning confocal microscopy confirms that the human corneal sub-basal nerve plexus is a highly dynamic structure. Invest Ophthalmol Vis Sci 2008;49:3409-12.
20. Edwards K, Pritchard N, Poole C, Dehghani C, Al Rashah K, Russell A, Malik RA, Efron N. Development of a Novel Technique to Measure Corneal Nerve Migration Rate. Cornea 2016;35:700-5.
21. Kim J, Markoulli M. Automatic analysis of corneal nerves imaged using in vivo confocal microscopy. Clin Exp Optom 2018;101:147-61.
22. Köhler B, Bretthauer G, Guthoff RF, Reichert K-M, Sieber I, Stachs O, Toso L, Allgeier S. EyeGuidance – a computer controlled system to guide eye movements. Current Directions in Biomedical Engineering 2016;2:433–6.
23. Allgeier S, Maier S, Mikut R, Peschel S, Reichert KM, Stachs O, Köhler B. Mosaicking the subbasal nerve plexus by guided eye movements. Invest Ophthalmol Vis Sci 2014;55:6082-9.
24. Kobayashi A, Yokogawa H, Sugiyama K. In vivo laser confocal microscopy of Bowman's layer of the cornea. Ophthalmology 2006;113:2203-8.
25. Yokogawa H, Kobayashi A, Sugiyama K. Mapping of normal corneal K-structures by in vivo laser confocal microscopy. Cornea 2008;27:879-83.
26. Bron AJ. Anterior corneal mosaic. Br J Ophthalmol 1968;52:659-69.
27. Bohn S, Stahnke T, Sperlich K, Linke SJ, Farrokhi S, Klemm M, Allgeier S, Köhler B, Reichert KM, Witt M, Stachs O, Guthoff RF. In vivo Histology of the Cornea

- from the "Rostock Cornea Module" to the "Rostock Electronic Slit Lamp" - a Clinical "Proof of Concept" Study. Klin Monbl Augenheilkd 2020;237:1442-54.
28. Bohn S, Sperlich K, Allgeier S, Bartschat A, Prakasam R, Reichert KM, Stolz H, Guthoff R, Mikut R, Köhler B, Stachs O. Cellular in vivo 3D imaging of the cornea by confocal laser scanning microscopy. Biomed Opt Express 2018;9:2511-25.
29. Allgeier S, Bartschat A, Bohn S, Peschel S, Reichert KM, Sperlich K, Walckling M, Hagenmeyer V, Mikut R, Stachs O, Köhler B. 3D confocal laser-scanning microscopy for large-area imaging of the corneal subbasal nerve plexus. Sci Rep 2018;8:7468.
30. Allgeier S, Bartschat A, Bohn S, Guthoff RF, Hagenmeyer V, Kornelius L, Mikut R, Reichert KM, Sperlich K, Stache N, Stachs O, Köhler B. Real-time large-area imaging of the corneal subbasal nerve plexus. Sci Rep 2022;12:2481.
31. Sterenczak KA, Stache N, Bohn S, Allgeier S, Köhler B, Bartschat A, George C, Guthoff RF, Stachs O, Stachs A. Burst of Corneal Dendritic Cells during Trastuzumab and Paclitaxel Treatment. Diagnostics (Basel) 2021;11:838.
32. Al Rashah K, Pritchard N, Dehghani C, Ruggeri A, Guimaraes P, Poole C, Russell A, Malik R, Efron N, Edwards K. Repeatability of Measuring Corneal Nerve Migration Rate in Individuals With and Without Diabetes. Cornea 2016;35:1355-61.
33. Chao C, Golebiowski B, Zhao X, Chen S, Zhou S, Stapleton F. Long-term Effects of LASIK on Corneal Innervation and Tear Neuropeptides and the Associations With Dry Eye. J Refract Surg 2016;32:518-24.
34. Chao C, Zhou S, Stapleton F, Chen S, Zhou X, Golebiowski B. The structural and functional corneal reinnervation mechanism at different regions after LASIK-an in vivo confocal microscopy study. Graefes Arch Clin Exp Ophthalmol 2022;260:163-72.
35. Lum E, Golebiowski B, Swarbrick HA. Changes in Corneal Subbasal Nerve Morphology and Sensitivity During Orthokeratology: Onset of Change. Ocul Surf 2017;15:227-35.
36. Lum E, Golebiowski B, Swarbrick HA. Reduced Corneal Sensitivity and Sub-Basal Nerve Density in Long-Term Orthokeratology Lens Wear. Eye Contact Lens 2017;43:218-24.
37. Al Rashah K, Pritchard N, Dehghani C, Ruggeri A, Guimaraes P, Russell A, Malik RA, Efron N, Edwards K. Corneal Nerve Migration Rate in a Healthy Control Population. Optom Vis Sci 2018;95:672-7.

Cite this article as: Stache N, Sterenczak KA, Sperlich K, Marfurt CF, Allgeier S, Köhler B, Mikut R, Bartschat A, Reichert KM, Guthoff RF, Stachs A, Stachs O, Bohn S. Assessment of dynamic corneal nerve changes using static landmarks by *in vivo* large-area confocal microscopy—a longitudinal proof-of-concept study. Quant Imaging Med Surg 2022. doi: 10.21037/qims-22-15